Journal of Power Sources 229 (2013) 285–298

Contents lists available at SciVerse ScienceDirect

Journal of Power Sources

journal homepage: www.elsevier.com/locate/jpowsour

Probabilistic model of polymer exchange fuel cell power plants for hydrogen, thermal and electrical energy management

Taher Niknam [a], Faranak Golestaneh [a], Ahmad Reza Malekpour [b,c,*]

[a] Department of Electrical and Electronic Engineering, Shiraz University of technology, Shiraz, Iran
[b] Young Researchers Club, Zarghan Branch, Islamic Azad University, Zarghan, Iran
[c] Department of Electrical and Computer Engineering, Kansas State University, Manhattan, KS 66506, USA

HIGHLIGHTS

- Consider the effect of hydrogen produced by PEMFC on MGs.
- Present an electrochemical model for PEMFC.
- Present a probabilistic model of PEMFC.
- Proposes a probabilistic economic/emission management of MGs.

ARTICLE INFO

Article history:
Received 6 September 2012
Received in revised form
20 October 2012
Accepted 16 November 2012
Available online 29 November 2012

Keywords:
Combined heating and power (CHP)
Hydrogen production
Micro grid (MG)
Multi-objective modified gravitational search algorithm (MGSA)
PEM fuel cell
Point estimate method

ABSTRACT

This paper proposes a probabilistic approach for economic/emission management of Micro Grids (MGs). In order to meet the electrical and thermal loads while having lower emission production in a more economical manner, combining heating and power along with hydrogen production and utilization strategies are employed. A PEMFCPP (Proton Exchange Membrane Fuel cell power plant) is considered as the prime mover of the Combined Heat and Power (CHP) system. The surplus power of PEMFCPP is managed to produce hydrogen. An electrochemical model for representation and performance evaluation of the PEMFC is applied. Using this model, the output voltage and power of the PEMFC are calculated as a function of current, constructive and operational parameters. The proposed probabilistic optimization method includes $2m + 1$ point estimate method to cover the uncertainties and a modified multi-objective algorithm based on the Modified Gravitational Search Algorithm (MGSA) to find Pareto-optimal front of the operation management problem. The study considers the uncertainties in forecasted values of: the hourly market tariffs, electrical and thermal load demands, available output power of the PhotoVoltaic (PV) and Wind Turbines (WT) units, fuel prices, hydrogen selling price, operation temperature of the FC, and pressure of the reactant gases of FC.

1. Introduction

Micro grids are clusters of distributed energy resource (DER) units located near the electrical and thermal loads, and can be organized to work in both grid-connected and autonomous modes [1]. The MGs offer a wide verity of benefits to the utility owners and customers such as [2]: dealing with environmental concern by reduction of carbon emissions because of using renewable energy sources and more efficient use of fossil fuels, energy efficiency improvement due to less line losses and co-generation options, increasing the power quality and reliability because of generating power near the loads, finally reducing investment risks and increasing fuel diversification. The DER units can be categorized into two concepts: the distributed generation (DG) and the distributed storage (DS) units. The DG units include several technologies such as FCs, micro turbines (MTs), diesel engines, PV and WTs. Likewise; the DS units contain batteries, energy capacitors, fly wheels and controllable loads [3].

Recently, FCs attract much attention due to their high efficiency, low aggression to the environment, vibration free, co-generation

* Corresponding author. Department of Electrical and Computer Engineering, Kansas State University, Manhattan, KS 66506, USA. Tel./fax: +1 785 226 3551.
E-mail addresses: niknam@sutech.ac.ir (T. Niknam), malekpour@ksu.edu (A.R. Malekpour).

0378-7753/$ – see front matter © 2012 Elsevier B.V. All rights reserved.
http://dx.doi.org/10.1016/j.jpowsour.2012.11.052

Nomenclature

Symbol, description

t, k time interval and iteration index, respectively
n total number of optimization variables
NT total number of hours
N_g, N_s total number of generation expect FCPP and storage units, respectively
N_D total number of load levels
$\tilde{f}(X)$ expected cost
u_i^t status of unit i at hour t
p_{Gi}^t, p_{sj}^t active power output of the generator i and the storage device j at time t, respectively
p_{Grid}^t active power bought/sold from/to the utility at time t
B_{Gi}^t, B_{sj}^t bid of the DG source i and the storage device j at hour t, respectively
B_{Grid}^t bid of utility at hour t
S_{Gi}, S_{sj} start-up/shut-down costs for the i DG unit and the storage device j, respectively
L_{elect}^t total electrical load at time t
$p_{Gi,\min}^t$, $p_{Gi,\max}^t$ minimum and maximum active power production of the DG unit i at hour t
$p_{sj,\min}^t$, $p_{sj,\max}^t$ minimum and maximum active power production of the storage j at hour t, respectively
$p_{grid,\min}^t$, $p_{grid,\max}^t$ minimum and maximum active power production of the utility at hour t, respectively
Res^t the scheduled spinning reserve at time t
$P_{cell,\max}$ maximum generating power limit of FCPP
B_{cell}^t price of natural gas for FCPP
B_{th}^t fuel price for residential thermal loads
B_{pump}^t hydrogen pumping cost
B_{Hs}^t hydrogen selling price
P_{cell}^t electrical power produced by FCPP in interval t
P_{Hst}^t stored hydrogen amount at interval t
P_H^t equivalent electric power for hydrogen production
$P_{H,end}$ available amount of hydrogen at the end of the day
$P_{H_usage}^t$ secondary hydrogen stream amount in kW at interval t
P_{Hst}^t stored hydrogen amount at interval t
α, β hot and cold start up cost of fuel cell, respectively
$electrical\eta$ electrical efficiency at full load
$thermal\eta$ thermal efficiency at full load
R_{elect} resistance to the electrons flow
R_{prot} equivalent membrane resistivity
z_l value of the lth input random variable of the $2m$ point estimate method
$z_{l,po}$ poth standard location of z_l
$\omega_{l,po}$ poth weighting factor $z_{l,po}$
μ_S, σ_S mean and the standard deviation of the S, respectively
N, Prob($z_{l,j}$) number of observations of z_l and the probability of each observation $z_{l,j}$, respectively
m number of the input random variables of $2m + 1$ point estimate method
$Iter_{\max}$ maximum number of iterations
r random number with uniform distribution between 0 and 1.
$Iter$ current iteration.
R_{je}^k Euclidian distance between two particles j and e.
ε small positive constant
N_{swrm} total number of the bees in the *swarm*
M_j^k, M_e^k gravitational mass related to particles j and e.
$V_{new,j}^{k,t}$, $V_{old,j}^{k,t}$ new and old velocity of the jth particle, respectively.
$X_{new,j}^{k,t}$, $X_{old,j}^{k,t}$ new and old position of the jth particle, respectively
G^k gravitational constant at the kth iteration
$Fit(\mathbf{X}_j^k)$ fitness value of the jth particle.
τ fuel cell cooling time constant
η_{cell}^t fuel cell efficiency at interval t
η_{st} hydrogen storage efficiency
L_{th}^t thermal load demand at interval t
r_{TE} thermal to electrical energy ratio
t_{off} time the FCPP has been off
i_{FC} cell operating current (A)
λ the ratio of the number of water moles for each sulfonic group in the membrane
T cell operation temperature (K)

List of abbreviations

MG micro grid
MGSA modified gravitational search algorithm
GSA gravitational search algorithm
DER distributed energy resource
DG distributed generation
DS distributed storage
WT wind turbine
MT micro turbine
PV photovoltaic
EEM economic/emission management
MGCC micro grid central controller
PEMFC proton exchange membrane fuel cell
FCPP fuel cell power plant
NiMH-battery nickel–metal-hydride battery
PDF probability density function
CDF cumulative density function
IRV input random variable
ORV output random variable
DM decision maker
STD standard deviation

options, superior reliability and modular nature [4]. In particular, PEMFCs emerge as a promising candidate for both stationary and automotive applications. The attractiveness of the PEMFCs in automotive applications is due to their high power density (about 0.5 W/cm^2) and low operating temperature (about 50–90 °C). The PEMFCs consume pure hydrogen as fuel and produce water as a by-product waste [5]. Typically one single cell produces about 0.5–0.9 V, so in power generating systems several cells are connected in series to create a stack which can provide hundreds of kilowatt [6]. Several studies have shown that in order to make the FCs more cost-effective it is necessary to recover waste thermal energy and manage producing hydrogen [7,8].

Hydrogen is one of the most environmental friendly and beneficial fuels which can operate as a storage medium or energy carrier. Reaction of hydrogen with oxygen produces water with no pollutant [9–11]. Generally, the production of hydrogen from fossil fuels is considered on an 'as needed' basis. However, sometimes it is more economical and efficient to store the hydrogen fuel as hydrogen [7]. In this regard, in order to make FCPPs more profitable, some amount of the reformer capacity can be employed to produce

hydrogen to be stored. The stored hydrogen can be reused to generate electricity by the FCs or to be sold to other customers. Moreover, recovering the waste thermal energy of the FCs to make a CHP system is one of the significant options to improve the FCs efficiency. More efficient energy used in the CHP systems leads to cost and fuel saving and consequently carbon emission reduction [12].

In the last few years, several researches have focused on environmental and economic concepts of the MGs, the CHP systems and hydrogen production. Chen et al. [3] presented a smart energy management system based on the matrix real-coded genetic algorithm to optimize the operation of the MGs. The proposed framework in Ref. [3] consists of a power forecasting module, an energy storage system management module and an optimization module. Hernandez et al. developed an optimization scheme to reduce the fuel consumption of the MGs while the local energy demand (both electrical and thermal) and a certain minimum reserve power were satisfied. Tsikalakis et al. optimized the operation of the MGs during inter-connected operation by optimizing the generation of the DG units and power exchange with the upstream network [13]. In Ref. [14], a linear programming was examined to minimize the average production cost of electric power in a hybrid solar-wind MG while environmental factors were considered. Moreover, in the filed of the FC micro CHP and hydrogen management, El-Sharkh et al. proposed an economic model for PEMFC and used an evolutionary-based technique to find an operational strategy for hydrogen utilization and waste thermal energy recovery [15]. The introduced model of the PEMFC in Ref. [15] is an imperfect one which doesn't consider the operation condition of the FC such as its operation temperature and pressure of reactant gases. Moreover, the aforementioned paper doesn't analyze environmental criterion. In Ref. [16], an experimental investigation of the PEMFC for both heat and power production was discussed and shown that utilization of the generated heat for domestic water heating could increase the efficiency of the FCs to about 70% in comparison with only 35–50% for electricity generation alone. In Ref. [17], an economic and environmental evaluation of two micro CHP alternatives, namely, gas engines and FC with different operating modes for residential buildings were proposed. The analyses demonstrate that the FC systems could select as a better options for the examined residential building from both environmental and economic points of view. Hawkes et al. devised a techno-economic model for the design and control of FCs micro CHP system and discussed the impact of the stack degradation on economic and environmental performances [18,19]. In Ref. [20], a comparison between the heat led and electricity led operation strategies for a residential micro CHP system was offered.

One of the drawbacks associated with previous studies for the operation management of the MGs is neglecting the uncertainty in generation patterns, load demand and market tariffs, fuel prices and operation condition of the FCs. The deterministic approaches are dependent on the accuracy of the input data, so errors in the input random data leads to unreliable solutions. In deed, some phenomena have uncontrollable nature or too implicit circumstance for being accurately modeled. The market tariffs, fuel prices and load demands, for example, regarding to open access market and divers customer types are more unpredictable than before [21–23]. Moreover, due to the stochastic nature of the wind speed and the solar radiation, the PV and WT units generate uncontrollable and fluctuated power. Therefore, the validity of the traditional optimization methods should be re-examined under new circumstance [13]. In this regard, from the system planning point of view, new approaches need to be employed for the economic/emission management (EEM) of the MGs to cope with the intermittency in input random data and minimize the risk associated with the design and operation under uncertainty [24,25]. This paper for handling the uncertainty organizes the EEM problem as a probabilistic one.

The probabilistic methods can be classified in three categories: the Monte Carlo Simulation (MCS) [26], the analytical techniques and the approximate methods. The MCS randomly generates several values for each input random variable (IRV) and solves the problem for each of them as a deterministic one. Although MCS can provide accurate solutions, its huge computational burden makes it unattractive and unacceptable for practical applications. Analytical techniques apply fewer numbers of simulations but require more assumptions and complicated mathematical computations [27]. Approximate methods provide a good balance between computational efficiency and accuracy [28]. The Point estimate method, as an approximate method, is an efficient and reliable method to model the uncertainty in power systems [19]. Mostly, the $2m$ point estimate method has been used to deal with power system problems. The $2m$ scheme generally fails to give satisfactory results when the number of uncertain input variables is high [25].

In this paper, the $2m + 1$ point estimate method is devised to optimize the energy management of MGs. The estimate points, in this method, are independence to the number of IRVs thus the $2m + 1$ scheme unlike the $2m$ one can provide satisfactory results in problems with a large numbers of uncertain inputs [25]. The $2m + 1$ scheme generates three values for each IRV and like the MSC solves the problem by deterministic routines for them. In this study, the hourly market tariffs, electrical and thermal load demand, available output power of the PV and WT units, fuel prices, operation temperature of the FC, pressure of the reactant gases of FC are considered as IRVs. The normal and beta probability density function (PDF) are used to model the variations of IRVs. Moreover, the Gram–Charlier expansion is employed to provide more accurate probability distribution for Output Random Variables (ORVs). An electrochemical-based FC model is used to calculate output power of the FC as a function of load current and membrane humidity. Furthermore, total operational cost and emissions of the MGs including emission and power production of different DG and DS units, trade with the market and hydrogen utilization management are formulated. The EEM model emphasizes a practical formulation of the PEMFC and links it to the economic and emission model. Finally, a multi-objective modified gravitational search algorithm (MGSA) is devised to optimize the EEM of the MGs.

The GSA is inspired by the law of gravity and mass interactions. In GSA method, the individuals are collection of masses which interact with each other using a policy inspired by the Newtonian gravity law and also the laws of motion [29]. This study takes advantages of the GSA and improves it to devise a powerful multi-objective optimization algorithm for solving the probabilistic EEM problem of the MGs. Firstly, in order to enhance the diversity of solutions, a mutation technique is suggested. It is expected this mutation to help the algorithm to escape being trapped into local optima. After that, the modified GSA is expanded to make a multi-objective one. Finally, the multi-objective MGSA is linked to $2m + 1$ point estimate method to find the uniformly POF of the probabilistic EEM problem with two conflicting objectives (cost and emission minimization). The effectiveness of the proposed technique is verified on a typical MG participates in the open market considering the FC, electrical and hydrogen storage, MT, PV and WT units and hydrogen production.

2. Operation management of a micro grid

2.1. Objective functions

2.1.1. Minimization of the total operating cost

The total operating cost of the MG includes the fuel costs of units as well as their start-up/shut-down costs. The objective function can be formulated as follows [15,30]:

$$\begin{aligned} Min f_1(\mathbf{X}) = \sum_{t=1}^{NT} Cost^t = \sum_{t=1}^{NT} \Bigg\{ & \sum_{i=1}^{N_g} \Big[u_i^t p_{Gi}^t B_{Gi}^t + Start_{Gi} \\ & \times \max\left(0, u_i^t - u_i^{t-1}\right) + Shut_{Gi} \times \max\left(0, u_i^{t-1} - u_i^t\right) \Big] \\ & + \sum_{j=1}^{N_s} \Big[u_j^t p_{sj}^t B_{sj}^t + Start_{sj} \times \max\left(0, u_j^t - u_j^{t-1}\right) + Shut_{sj} \\ & \times \max\left(0, u_j^{t-1} - u_j^t\right) \Big] + P_{Grid}^t B_{Grid}^t \\ & + B_{cell}^t \left((P_{cell}^t + P_H^t) / \eta_{cell}^t \right) B_{th}^t \times \max(L_{th}^t - P_{th}^t, 0) \\ & + B_{pump}^t \eta_{st} P_H^t \Bigg\} + \alpha + \beta\left(1 - \exp\left(t_{off}/\tau\right)\right) - B_{Hs} P_{H,end} \\ & + OM \end{aligned} \tag{1}$$

where $\mathbf{X} = [X^1 X^2 \ldots X^t \ldots X^{NT}]$ and X^t is design variables vector including active powers of units and their related states that can be described as follows:

$$X^t = \left[p_{G1}^t, p_{G2}^t, \ldots, p_{GNg}^t, P_{Grid}^t, P_{cell}^t, P_H^t, P_{th}^t, p_{s1}^t, p_{s2}^t, \ldots, p_{sNs}^t, u_1^t, u_2^t, \ldots, u_{Ns+Ng+2}^t \right]^T \tag{2}$$

2.1.2. Minimization of the total pollutants emissions

In this study, the environmental effects of carbon dioxide (CO_2), sulfur dioxide (SO_2) and nitrogen oxides (NO_x) are involved in the optimization problem. Mathematical functions which formulate emissions associated with the power production of different DG units are employed. The second objective can be described as follows:

$$\begin{aligned} Min f_2(\mathbf{X}) = \sum_{t=1}^{T} Emission^t = \sum_{t=1}^{T} \Bigg\{ & \sum_{i=1}^{N_g} \left[u_i^t p_{Gi}^t E_{Gi}^t \right] + \sum_{j=1}^{N_s} \left[u_j^t p_{sj}^t E_{sj}^t \right] \\ & + p_{Grid}^t E_{Grid}^t \Bigg\} \end{aligned} \tag{3}$$

where E_{Gi}^t, E_{sj}^t and E_{Grid}^t define the amount of emissions in kg/kWh for each DG, storage unit and the utility at hour t respectively. These variables are expressed as follows:

$$E_{unit_e}^t = CO_{2_{unit_e}}^t + SO_{2_{unit_e}}^t + NO_{x_{unit_e}}^t \tag{4}$$

where $CO_{2_{unit_e}}^t$, $SO_{2_{unit_e}}^t$, $NO_{x_{unit_e}}^t$ and $E_{unit_e}^t$ are the amounts of carbon dioxide, sulfur dioxide and nitrogen oxides emissions from unit e (DG/DS/utility) at hour t, respectively.

2.2. Constraints

- Power balance:

$$\sum_{i=1}^{N_g} p_{Gi}^t + \sum_{j=1}^{Ns} p_{sj}^t + P_{Grid}^t + P_{cell}^t + P_{H\_usage}^t = L_{elect}^t \tag{5}$$

- Real power generation capacity:

$$\begin{aligned} & p_{Gi,\min}^t \le p_{Gi}^t \le p_{Gi,\max}^t \\ & p_{si,\min}^t \le p_{si}^t \le p_{si,\max}^t \\ & P_{grid,\min}^t \le P_{Grid}^t \le P_{grid,\max}^t \\ & P_{cell,\min} \le P_{cell}^t + P_H^t \le P_{cell,\max} \end{aligned} \tag{6}$$

- Spinning reserve:

$$\sum_{i=1}^{N_g} u_i^t p_{Gi,\max}^t + \sum_{j=1}^{Ns} u_j^t p_{sj,\max}^t + P_{grid,\max}^t + P_{cell,\max}^t \ge L_{elect}^t + Res^t \tag{7}$$

3. CHP system

In this study, PEMFC is considered as a prime mover of CHP system. The PEMFC consumes pure hydrogen as its fuel; transform the chemical energy liberated during the electrochemical reaction of hydrogen and oxygen to electrical energy and produce zero emissions besides water vapor. Typical configuration of a PEMFC can be found in Fig. 1 [5]. Separation of hydrogen from

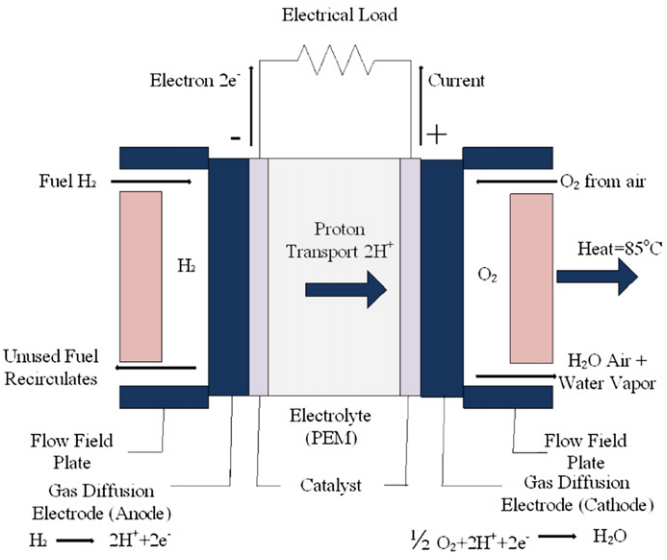

Fig. 1. Basic PEMFC operation.

hydrocarbons is carried out through an exothermic reaction known as reforming and is done by reformers. It's assumed that some amount of produced hydrogen by reformer is stored for further usage also a part of local thermal loads are satisfied by recovered thermal energy of the reformer.

3.1. Hydrogen production strategy

As shown in Fig. 2, the generated power of the reformer divided into two parts. One of them, by the main hydrogen stream enters to the stack; while the other part is stored in the hydrogen tank for further utilization. In order to take account of the later part of the generated hydrogen in the PEMFC model an equivalent electrical power is attributed to it asP_H [15]. In this study, P_H is considered as one of the design variables and its value can change in the range of zero and P_{Diff}, where $P_{Diff}$is defined as:

$$P_{Diff} = P_{cell,\max} - P_{cell} \tag{8}$$

As in this paper, the recovered energy of the reformer is used for co-generating, in high thermal demand intervals which reformer works in high capacity to satisfy thermal load demands as much as is economical, some amount of the generated hydrogen are stored in the hydrogen tank. The stored hydrogen in addition to the hydrogen produced by the reformer can be used in the low thermal demand intervals to generate the required electrical power. The unused hydrogen in the hydrogen tank is sold at the end of the day. The hydrogen production in kg/s can be computed as follows [15]:

$$H_2(Amount) = 1.05 \times 10^{-8} \times \left(\frac{P_H}{V_{FC}}\right) \tag{9}$$

The stored hydrogen amount in the hydrogen tank can be calculated as follows:

$$P^t_{Hst} = P^{t-1}_{Hst} + P^t_H \times \eta_{st} - P^t_{H_usage} \tag{10}$$

It is anticipated that this policy makes the operation management of the MG more economical and improves the efficiency of the FCPP. In this paper, the hydrogen storage cost is assumed equal to the pumping cost and no storage infrastructure or technology cost is taken to account.

3.2. Recovered thermal energy FCPP

This work recovers the waste heat generated by the reformer in order to make a CHP system and satisfy some amount of the MG thermal loads by recovered thermal energy. It is expected that the CHP systems provide a higher thermal efficiency in comparison with producing heat and power separately; consequently for the same output, less fuel is consumed which causes to reduce the operational cost and emissions of greenhouse gases [31]. The recovered thermal power from the FCPP can be computed as:

$$P^t_{th} = r_{TE} \times (P^t_H + P^t_{cell}) \tag{11}$$

where r_{TE} along with the efficiency of the cell η^t_{cell} are function of PLR (PLR = electrical generated power/maximum power) [15]. Recovering the thermal power and the hydrogen management improve the overall efficiency of the cell greatly. The overall efficiency can be given as [15]:

$$\eta^t_{overall} = \frac{P^t_{cell} + \eta_{st} \times P^t_H + \min(P^t_{th}, L^t_{th})}{\frac{P^t_{cell} + P^t_H}{\eta^t_{cell}}} \tag{12}$$

Moreover, Thermal and electrical efficiencies at full load can be defined by the following formula [32,33]:

$$electrical\eta = \frac{P_{cell} + \eta_{st} \times P_H}{P_{in}} \tag{13}$$

$$thermal\eta = \frac{\min(P_{th}, L_{th})}{P_{in}} \tag{14}$$

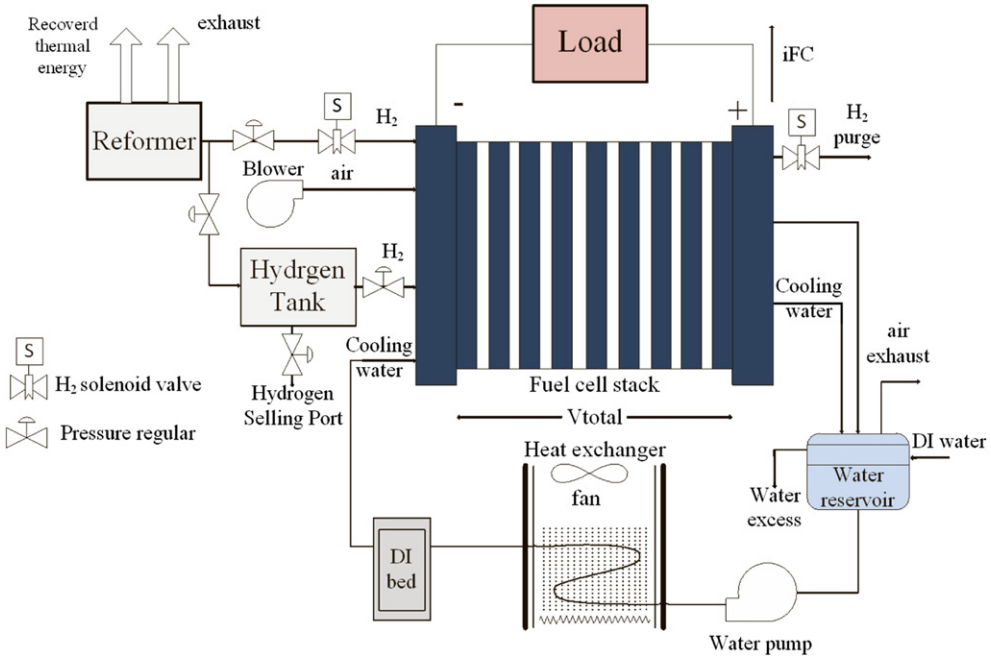

Fig. 2. Generation system with PEMFC stacks.

4. 2m + 1 point estimate method

This paper employs $2m+1$ point estimate method to cover the uncertainty in forecasted values of electrical and thermal load demands, available output power of the PV and WT units, market prices in each interval, natural gas price for the FCPP, operation temperature of the FC, pressure of the reactant gases of FC, fuel price for those thermal loads of the MG which are not satisfied by the FCPP and hydrogen selling price.

Firstly, the point estimate method was introduced by Rosenblueth in 1975 [34] but there is a significant drawback associated with Rosenblueth's method and that is their heavy computational burden requirement. In 1989, Harr developed a new point estimate method to overcome the drawback of Rosenblueth's method [35]. Although the Harr's method was computationally more efficient than the prior ones, it was restricted to symmetric variables. In 1998, Hong introduced a new point estimate method which was computational more efficient than the previous ones [36]. The Hong's method is suitable for both symmetric and asymmetric variables. This paper proposes the Hong's $2m+1$ point estimate method to solve the probabilistic EEM problem of the MGs. Mostly, the Hong's $2m$ point estimate method has been used in the literature for power system problems. The $2m+1$ scheme is more accurate than the $2m$ one for two reasons. First, the $2m+1$ scheme considers both skewness and kurtosis of IRVs while the $2m$ scheme doesn't use the second one. In addition, the estimated points in the $2m+1$ scheme unlike those in the $2m$ one are independent to the number of IRVs, so in problems with a large numbers of uncertain variables again it can be an efficient method. It is worth mentioning that, the $2m+1$ scheme needs only one additional evaluation of the objective function in composition with the $2m$ scheme.

The Deterministic optimal planning of the MGs depends on a set variables v such as output power of different units, load demands and market prices as:

$$S_{ORV} = f(v) \tag{15}$$

where $S_{ORV}(ORV = 1,2)$ are the outputs of optimal planning and f is the set of operation cost and emission equations.

In the deterministic EEM of an MG, the aforementioned variables have fixed values but in realty, some of those variables are uncertain. For example, there are always errors in forecasted values for the output power of the WTs, the PVs or the market price and the load demands. The function f transfers the uncertainty from the IRVs to the ORVs as follows:

$$S_{ORV} = f(c, z_1, z_2, \ldots, z_m) \tag{16}$$

where c is the set of certain variables, $z_l(l = 1,\ldots,m)$ are input variables under uncertainty and S_{ORV} are the outputs of optimal planning.

The goal of the $2m+1$ scheme is finding the statistical information of the ORVs by using the first few central moments of the IRVs i.e. the mean μ_{p_l}, variance σ_{p_l}, skewness $\lambda_{p_l,3}$ and kurtosis $\lambda_{p_l,4}$ coefficients. Employing just first few central moments of IRVs to evaluate the characteristics of the output set is a remarkable advantage of the point estimate methods where implementing the features of IRVs is difficult task to reach.

The$2m+1$ method produces two probability concentration for each IRV z_l as $(z_{l,1}, w_{l,1})$ and$(z_{l,2}, \omega_{l,2})$. The$z_{l,po}(po = 1,2)$ is called the poth location of z_l and $\omega_{l,po}(po = 1,2)$ is a weighting factor which specifies the importance of the corresponding location in evaluating the statistical moments of the ORVs. The deterministic EEM problem is simulated $2m+1$ times in the proposed probabilistic method. One of the mentioned simulations is done by fixing all the IRVs on their mean values called Mean location while in each of the $2m$ reaming simulations, one of the IRV is fixed to one of its locations, and the other IRVs are equal to their mean values as follows:

$$S_{ORV(l,po)} = f\left(c, \mu_{z_1}, \mu_{z_2}, \ldots, z_{l,po}, \ldots, \mu_{z_m}\right), \quad po = 1,2 \quad l = 1,2,\ldots,m \tag{17}$$

where c is the set of certain variables, $z_{l,1}$ and $z_{l,2}$ are the specified locations of the IRV z_l and μ_{z_l} is the mean value of the left over IRVs. Once the solutions of $2m+1$ deterministic EEM are explored, using the weighting factors the first and the second moments of each ORVs can be estimated.

The step by step procedure of $2m+1$ point estimate method to calculate the moments of the ORVs can be summarized as

Step 1: Define$m$.
Step 2: Set $E(S_{ORV}^h) = 0$, $h = 1, 2$.
Step 3: Select an uncertain parameterz_l.
Step 4: Calculate the skewness $(\lambda_{z_l,3})$ and the kurtosis $(\lambda_{z_l,4})$ of the z_l according to the following equations:

$$\lambda_{z_l,3} = \frac{E\left[(z_l - \mu_{z_l})\right]^3}{(\sigma_{z_l})^3} \left(E\left[(z_l - \mu_{z_l})^3\right] = \sum_{j=1}^{N} \left(z_{l,j} - \mu_{z_l}\right)^3 \times \mathrm{Prob}\left(z_{l,j}\right) \right) \tag{18}$$

$$\lambda_{z_l,4} = \frac{E\left[(z_l - \mu_{z_l})^4\right]}{(\sigma_{z_l})^4} \left(E\left[(z_l - \mu_{z_l})^4\right] = \sum_{j=1}^{N} \left(z_{l,j} - \mu_{z_l}\right)^4 \times \mathrm{Prob}\left(z_{l,j}\right) \right) \tag{19}$$

Step 5: Calculate two standard locations:

$$\xi_{l,po} = \frac{\lambda_{z_l,3}}{2} + (-1)^{3-po} \sqrt{\lambda_{z_l,4} - \frac{3}{4}\lambda_{z_l,3}^2}, \quad po = 1,2 \tag{20}$$

Step 6: Compute two estimated location:

$$z_{l,po} = \mu_{z_l} + \xi_{z_l,po} \cdot \sigma_{z_l}, \quad po = 1,2 \tag{21}$$

Step 7: Calculate the deterministic EEM for the poth estimated location:

$$S_{ORV(l,po)} = f\left(c, \mu_{z_1}, \mu_{z_2}, \ldots, z_{l,po}, \ldots, \mu_{z_m}\right), \quad po = 1,2 \quad l = 1,2,\ldots,m \tag{22}$$

Step 8: Compute two weighting factors of z_l:

$$\omega_{l,po} = (-1)^{3-po} / \xi_{l,po}(\xi_{l,1} - \xi_{l,2}), \quad po = 1,2 \tag{23}$$

Step 9: Update the first and second moment of the ORVs (total operational cost and emission):

$$E\left(S_{ORV}^{h}\right) = E\left(S_{ORV}^{h}\right) + \sum_{po=1}^{2} \omega_{l,po} \cdot \left(S_{ORV(l,po)}\right)^{h}, \quad h = 1,2 \tag{24}$$

Step 10: Repeat steps 3–9 until all uncertain parameters were taken into account.
Step 11: Compute the weight factor of the mean location as follows:

$$\omega_{\mu} = 1 - \sum_{l=1}^{m} 1 \Big/ \left(\lambda_{l,4} - \lambda_{l,3}^{2}\right) \tag{25}$$

Step 12: Calculate the deterministic EEM for the mean location as:

$$S_{ORV,\mu} = f\left(c, \mu_{z_1}, \mu_{z_2}, \ldots, \mu_l, \ldots, \mu_{z_m}\right), \quad l = 1,2,\ldots,m \tag{26}$$

Step 13: compute the first and second moment of the *ORV* using ω_{μ} andS_{μ}:

$$E\left(S_{ORV}^{h}\right) = E\left(S_{ORV}^{h}\right) + \omega_{\mu} \cdot \left(S_{ORV,\mu}\right)^{h}, \quad h = 1,2 \tag{27}$$

Step 14: Compute the mean and standard deviation of the total operational cost and emission.

$$\mu_S = E\left(S_{ORV}^{1}\right), \quad \sigma_S = \sqrt{E\left(S_{ORV}^{2}\right) - \left(E\left(S_{ORV}^{1}\right)\right)^{2}} \tag{28}$$

The probability density function of each ORV can be approximated and plotted using its calculated mean and standard deviation and also Gram–Charlier series approach [37].

5. Modified GSA

5.1. Overview of standard GSA

The GSA has inspired by the Newton's law of gravity introduced in 2009 [29]. The gravitation, as one of the fundamental interactions in the nature, is the tendency of objects to accelerate toward each other. According to the law of gravity, each mass attracts every other one with a 'gravitational force'. The gravitational force between two particles is directly proportional to the product of their masses and inversely proportional to the square of the distance between them. Moreover, based on the Newton's second law, the acceleration of each particle only depends on the overall force acts on it and its mass [38]. In the GSA, the individuals are a collection of objects also the solutions of the problem and their corresponding fitness values are attributed to the positions and masses of those objects. The GSA expresses the gravitational force as follows:

$$F_{je}^{k,t} = G^{k} \times \frac{M_j^{k} \times M_e^{k}}{R_{je}^{k} + \varepsilon} \times \left(X_j^{k,t} - X_e^{k,t}\right) \tag{29}$$

where the gravitational constant decreases during the optimization process as:

$$G^{k} = G_o \times \exp\left(\varpi \times \frac{Iter}{Iter_{\max}}\right) \tag{30}$$

where G_o and ϖ are two constant which are set to 100 and 20, respectively [29].

The value of mass of each particle is computed by mapping its fitness value as the following equations:

$$m_j^{k} = \frac{Fit(\mathbf{X}_j^{k}) - worst^{k}}{best^{k} - worst^{k}} \tag{31}$$

$$M_j^{k} = \frac{m_j^{k}}{\sum_{e=1}^{N_{swrm}} m_e^{k}} \tag{32}$$

where $worst^{k}$ and $best^{k}$ are the maximum and the minimum fitness values at iteration k (in minimization problems).

The overall gravitational force exerted on the jth particle is calculated by a randomly weighted sum of forces applied by the other particles as follows:

$$F_j^{k,t} = \sum_{e=1, e\neq j}^{N_{swrm}} r_e \times F_{je}^{k,t} \tag{33}$$

The random parameter r_e is added to (33) to give the algorithm stochastic characteristics. The acceleration of each particle is defined as follows:

$$a_j^{k,t} = \frac{F_j^{k,t}}{M_j} \tag{34}$$

Finally, the new position and velocity of each particle are updated by the following equations:

$$V_{new,j}^{k,t} = a_j^{k,t} + r \times V_{old,j}^{k,t} \tag{35}$$

$$X_{new,j}^{k,t} = X_{old,j}^{k,t} + V_{new,j}^{k,t} \tag{36}$$

In order to balance the exploration and exploitation capability of the GSA, only a set of the particles with better fitness values, i.e. bigger mass, are selected to apply their forces to the others. Hence, (33) can be rewritten as:

$$F_j^{k,t} = \sum_{e\in kbest, e\neq j} r_e \times F_{je}^{k,t} \tag{37}$$

where *kbest* is a set of the particles with best fitness values. The number of the particles in *kbest* is a function of time which starts with N_{swrm} and decreases linearly to 1.

Analyzing the GSA algorithm, the following points can be deduced:

1. In GSA algorithm, it is expected that particles are attracted by the heaviest (i.e. most optimal) one because the heavier masses exert more powerful gravitational force according to (29).
2. As discussed before, according to the Newton's law, the gravitational force between two particles j and e is inversely proportional to the $(R_{je})^2$ while in (29), $R_{je}$is used instead of $(R_{je})^2$. It is because after several experiments it is found that this displacement provides better solutions [29].
3. Considering (34), the inertia mass tends to make the mass movement slow, so the motion of the heavier masses corresponded to the better solutions is more slow than the lighter ones. Thus, the GSA algorithm searches the space around the

optimal solutions more carefully which enhances the exploitation and local search capability of the algorithm.

4. The gravitational constant is employed to make balance between exploration and exploitation. It has a big value at the beginning to improve the exploration power of the algorithm and help to avoid being trapped in local optima. Also, it decreases during the optimization process to search the space with the higher probability of the optimal solution occurrence accurately.

5.2. Mutation

This paper proposes a mutation technique to improve the convergence characteristics of the original GSA. This mutation technique is proposed to improve the diversity of the solutions, alleviate the stagnation and avoid being trapped in local optima. For each particle, three particles are selected randomly as $n_1 \neq n_2 \neq n_3 \neq j$, and a trial solution is created as:

$$X_{trail}^{k,t} = X_{new,n_1}^{k,t} + r \times \left(X_{new,n_2}^{k,t} - X_{new,n_3}^{k,t}\right) \tag{38}$$

Using the following scheme, a mutant solution is achieved:

$$x_{mut,j\theta}^{t} = \begin{cases} x_{trial,j\theta}^{k,t} & \text{if } (r_1 \leq r_2) \\ x_{new,j\theta}^{k,t} & \text{else} \end{cases} \tag{39}$$

where $\theta = 1, 2, \ldots, n$ and r_1 and r_2 are two random numbers with normal distribution between 0 and 1. Finally, for each object, between the mutant position and position found by the original GSA, the one with the better fitness value is selected to participate in the next generation.

6. Multi-objective MGSA

Multi-objective optimization algorithms are devised to solve optimization problems with several incommensurable and conflicting objectives stimulatingly. These algorithms, instead of one single solution as optimal solution, provide a set of solutions named Pareto-optimal solutions. In absence of the any preferable information, each solution in this set has no priority over the others. The Pareto-optimal solutions are selected from the non-dominated solutions. To know the non-domination concept, suppose that $\mathbf{X}_1$ and $\mathbf{X}_2$ are two optimal solutions for a given multi-objective problem, $\mathbf{X}_1$ dominates $\mathbf{X}_2$ if and only if the following two conditions are satisfied:

$$\begin{array}{ll} \forall l \in \{1, 2, \ldots, n_o\}, & f_l(\mathbf{X}_1) \leq f_l(\mathbf{X}_2) \\ \exists q \in \{1, 2, \ldots, n_o\}, & f_q(\mathbf{X}_1) < f_q(\mathbf{X}_2) \end{array} \tag{40}$$

This paper employs the MGSA and develops it to devise a powerful multi-objective algorithm to solve the EEM of the MGs with two conflicting objectives as emission and cost minimization. To do this, several metaheuristic techniques are used to find uniformly POF including extreme points of the trade of surface. Firstly, an external archive, named Repository, is planned to store the non-dominated solutions. Each solution found by the algorithm is compared with the other ones also the repository members for non-domination and the non-dominated solutions are stored in the repository.

In order to determine the best compromise solution, a fuzzy approach is used in this paper. In the fuzzy approach, a fuzzy membership function is allocated to each of the objective functions as follows:

$$\mu_{f_n}(\mathbf{X}) = \begin{cases} 1, & f_n(\mathbf{X}) \leq f_n^{\min} \\ 0, & f_n(\mathbf{X}) \geq f_n^{\max} \\ \dfrac{f_n^{\max} - f_n(\mathbf{X})}{f_n^{\max} - f_n^{\min}}, & f_n^{\min} \leq f_n(\mathbf{X}) \leq f_n^{\max} \end{cases} \tag{41}$$

The DM's preference is defined by weight factors which are allocated to the objectives then the normalized membership value for each solution is calculated as:

$$N\mu(j) = \frac{\sum_{n=1}^{n_o} w_n \times \mu_{f_n}(\mathbf{X}_j)}{\sum_{j=1}^{m} \sum_{n=1}^{n_o} w_n \times \mu_{f_n}(\mathbf{X}_j)} \tag{42}$$

The number of the Pareto-optimal solutions of the problem may be excessive or even infinitive. Large size of the Pareto-optimal solution causes computational burden increase. Furthermore, there is always memory constraint. This paper uses the clustering approach to decrease the repository members without destroying its characteristics [39].

7. Solution methodology

7.1. The procedure for implementing the probabilistic multi-objective MGSA can be summarized in the following steps

Step 1: Randomly generate the initial positions of the particles in the feasible range (6).
Step 3: Implement the $2m + 1$ scheme. Calculate the first and the second moments of the total operation cost and emissions.
Step 4: Initialize the repository by storing the non-dominated solutions of the initial population.
Step 5: Sort the particles based on their first moment values. Thereafter, determine $worst^k$ and $best^k$.
Step 6: Update the gravitational mass of each particle M_j^k using (31) and (32).
Step 7: Update the overall force which is applied on each particle using (37).
Step 8: Calculate the acceleration and the velocity of each particle using (34) and (35).
Step 9: Update the particles position using (36).
Step 10: Implement the $2m + 1$ scheme as Step 3.
Step 11: Check for non-domination. Update the repository.
Step 12: Apply the mutation approach. Find the new solution for each particle.
Step 13: Implement the $2m + 1$ scheme as Step 3.
Step 14: Check for non-domination. Update the repository.
Step 15: Go to Step 4 until the current iteration number reaches the pre-specified maximum iteration number.

8. Simulation results

The MG considered in this paper consists of different DG units such as an MT, FCPP, PV, and WT. It is supposed that all DG units produce active power at unity power factor, neither requesting nor producing reactive power. Furthermore, there is a power exchange link between the mentioned MG and the utility (LV network) in order to trade energy during a day based on decisions of the Micro Grid Central Controller (MGCC).

Table 1offers different parameters used in this paper [4,15,30]. Parameters of the FC stack presented in Table 1 are adopted from Ref. [4]. The prices of DER units are considered as presented in Ref. [30] while the prices related to FCPP are estimated by scaling data given in Ref. [15]. The normalized forecasted output power of WT and PV units and the hourly forecasted market prices for a typical day can be found in Refs. [30,40]. The hourly electrical and

Table 1
Simulation parameters.

Parameter	Value
T	333 K
A	64 cm^2
l_M	178 μm
P_{H_2}	1 (atm)
P_{O_2}	0.2095 (atm)
B	0.016
R_C	0.0003
ξ_1	−0.948
ξ_2	$0.00286 + 0.0002 \ln(A) + \ln(C_{H_2})$
ξ_3	7.6×10^{-5}
ξ_4	-1.93×10^{-4}
J_{max}	469 mA cm^{-2}
I_{max}	30 A
Min, max power of FCPP	10, 250 (kW)
Min, max power of MT	10, 80 (kW)
Min, max power of PV	0, 45 (kW)
Min, max power of WT	0, 35 (kW)
Min, max power of Utility	−95, 95 (kW)
Price of natural gas for FCPP	0.21 (€ct/kWh)
Fuel price for residential loads	0.29 (€ct/kWh)
Hydrogen selling price	9.44 (€ct/kWh)
Hydrogen storage efficiency	0.95(€ct/kg)
Hydrogen pumping cost	0.09 (€ct/kWh)
The fuel cell cooling time constant	0.75
Hot start up cost	0.26 (€ct)
Cold start up cost	0.7 (€ct)
Bid of MT	0.457 (€ct/kWh)
Bid of PV unit	2.584 (€ct/kWh)
Bid of WT	1.073 (€ct/kWh)
N_{swrm}	40
$Iter_{max}$	300

thermal load profiles are adopted from Ref. [15]. Furthermore, if the recovered thermal energy from the reformer is not enough to satisfy the thermal load (cooling, heating, or hot water) additional heat has to be provided by an auxiliary boiler of the CHP system. The data for the auxiliary boiler can be found in Ref. [31]. Finally, Table 2 presents emission coefficients of different DER units [30,41].

In the following subsections, firstly, in order to show the effects of hydrogen production in the EEM problem, deterministic analysis are performed under two scenarios. In the first scenario S_1, no hydrogen is produced while in the second one S_2, hydrogen production strategy is employed. The multi-objective EEM problem is solved for both mentioned scenarios and the results in terms of the both cost and emission reductions are analyzed in detail. Finally, the probabilistic multi-objective MGSA is employed to find the POF of the probabilistic EEM problem with the hydrogen production strategy.

8.1. Deterministic analysis

In the deterministic EEM of the MGs, it is assumed that the output powers of the WT and the PV units are equal to their forecasted values and the remaining part of the load demand is satisfied by the other DG units. Moreover, market prices in each interval, natural gas price for the FCPP, operation temperature of the FC, pressure of the reactant gases of the FC, fuel price for the local thermal loads which are not satisfied by the FCPP and hydrogen selling price are considered to be equal to their expected values.

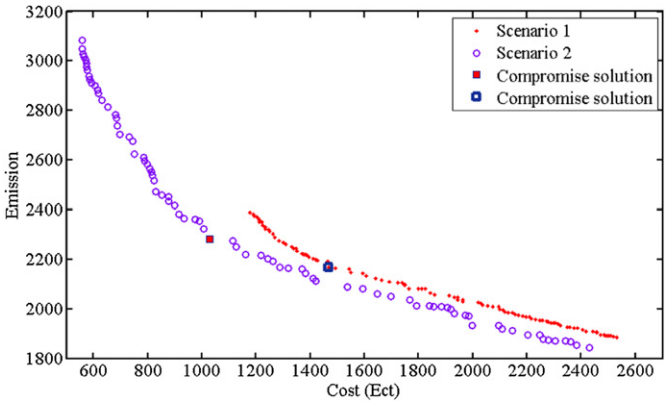

Fig. 3. POF of the deterministic EEM problem for both scenarios.

Deterministic multi-objective MGSA is used to find the POF of the EEM problem of the mentioned MG under aforesaid scenarios. The obtained POF for both S_1 and S_2 along with their best compromise solutions are portrayed in Fig. 3. It should be noted that in finding best compromise solutions, it is assumed that the DM's preference is unbiased, that is to say both w_1 and w_2 are equal to 0.5. As shown Fig. 3, great improvement in terms of the both cost and emission reduction using the hydrogen production and storage strategy is evident. The POF of the S_2 is well-distributed in the cost-emission space. Referring Fig. 3, for equal cost, S_2gives lower emission in comparison with S_1, at the same time, for equal emission for both S_1 and S_2, S_2 provides lower amount of emissions. As can be seen in Fig. 3, the superiority of the S_2 over S_1 is more manifest in cost minimization. For more convenience, Table 3 tabulates the extreme points of the trade-off surface also the best compromise solutions for both S_1 and S_2. By analyzing Table 3, hydrogen utilization management can save \$621.7 in per day. It is worthwhile noting that the thermal and electrical load profiles are given as spring/fall loads in Ref. [15], so the proposed hydrogen management can save about \$111,906 in spring and fall seasons which is surely noteworthy. In addition, when emission minimization is the goal of the MGCC, hydrogen management saves 100 kg daily and so, 18,000 kg for both spring and fall seasons. When the DM's preference is unbiased S_2 saves \$439.7 while its produced emission is just 114.26 kg more than S_1. Moreover, with the same cost (\$1466.84) for both S_1 and S_2, well hydrogen production management can reduce 60 kg emission production. For further discussion about how hydrogen utilization strategy makes remarkable profit for MGs, Figs. 4–9 are offered. Fig. 4 portrays thermal load of the MG, recovered thermal power of the reformer and generated power of the DG units for the power management corresponding to the minimum cost using S_1. Fig. 5 shows the same data for the power management corresponding to the minimum emission (S_1). Moreover, Fig. 6 gives the hourly data of

Table 2
Emission coefficient of the DG sources.

ID	Type	CO_2 (kg/MWh)	SO_2 (kg/MWh)	NO_x (kg/MWh)
1	MT	720	0.0036	0.1
2	FCPP	502.4780	0.0036	0.5215
3	PV	0	0	0
4	WT	0	0	0
6	Utility	921.0585	3.5827	2.2947

Table 3
Comparison of operational cost and emission of scenarios 1 and 2.

Method		Best cost	Best emission	Compromise solution
Scenario 1	Cost (€ct)	1179.29	2518.74	1466.84
	Emission (kg)	2391.08	1889.69	2.16952
Scenario 2	Cost (€ct)	557.53	2418.63	1027.14
	Emission (kg)	3083.46	1844.24	2283.78

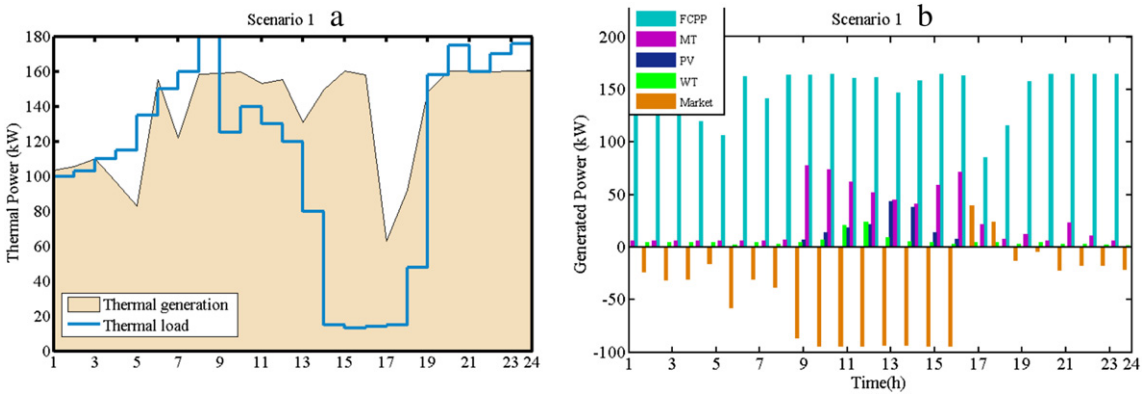

Fig. 4. Minimum cost – (a) thermal load of the MG and recovered thermal power, (b) generated power of DER units.

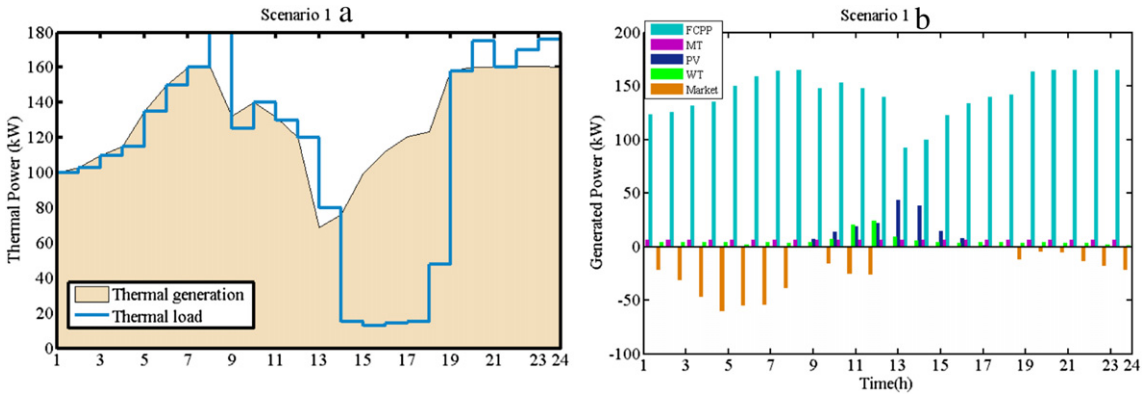

Fig. 5. Minimum emission – (a) thermal load of the MG and recovered thermal power, (b) generated power of DER units.

thermal load power and thermal generated power by the reformer (Fig. 6a), hydrogen equivalent production (Fig. 6b), the secondary hydrogen stream amount (Fig. 6c) and the stored hydrogen (Fig. 6d) over a 24 h period for the power and hydrogen management corresponding to minimum cost (S_2). In addition, Fig. 7 demonstrates the same data for the management with the minimum emission production. Figs. 8 and 9 show the generated power of the DG units for minimum cost and emission, respectively, when S_2 is

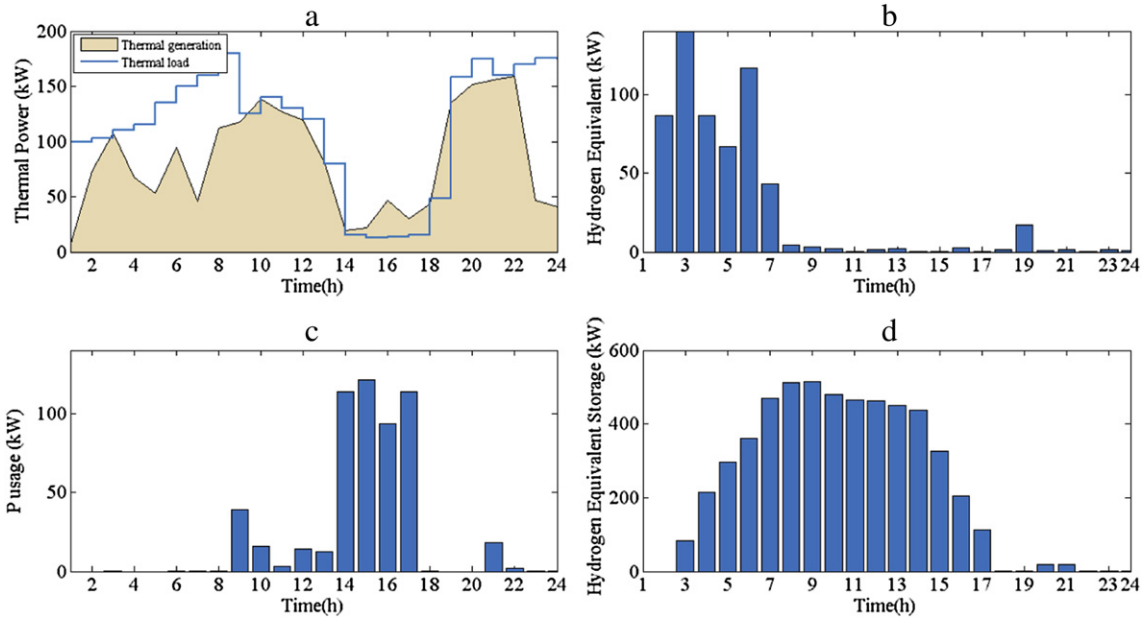

Fig. 6. Minimum cost – (a) thermal load and recovered. (b) Hydrogen production. (c) Secondary hydrogen stream amount. (d) Hydrogen equivalent storage.

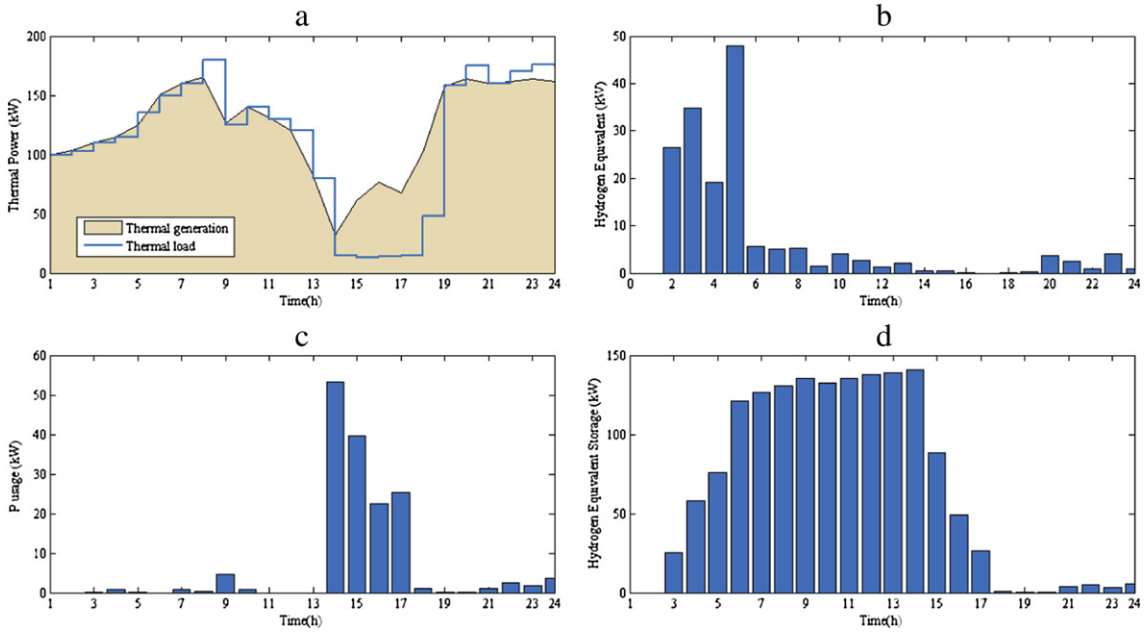

Fig. 7. Minimum emission – (a) thermal load and recovered. (b) Hydrogen production. (c) Secondary hydrogen stream amount. (d) Hydrogen equivalent storage.

employed. The idea behind the hydrogen management strategy is storing hydrogen in high thermal load intervals and using it along with hydrogen produced by the reformer to generate electrical power in low thermal demand intervals. Figs. 6 and 7 in comparison with Figs. 4 and 5 clearly show that the proposed methodology successfully follows the aforementioned strategy. As can be seen in the same figures, the MG experiences low thermal load between 14 pm and 18 pm. In S_1, during 14 pm–18 pm, in order to satisfy electrical load, the reformer is forced to produce hydrogen for the FCPP. Producing hydrogen is followed by producing heat which is more than the heating requirements of the MG, so the surplus of the thermal power to the MG's thermal requirement will be wasted. This fact causes lose money and generating more emissions. On the other hand, by handling hydrogen utilization, the MGCC can achieve more profitable management. As Figs. 6 and 7 demonstrate, in the first hours of the day which MG experiences low electrical load, the reformer is forced to produce more hydrogen than is required for FCPP and store it in the hydrogen tank. The stored hydrogen is used in the low thermal load intervals, more between 14 pm and 18 pm, to supply electrical load demand. By this policy, in low thermal load intervals the reformer doesn't have to produce hydrogen near to its rated capacity to supply electrical load which causes to waste some amounts of its generated heat. Moreover, Fig. 8 in comparison with Fig. 4 shows that hydrogen management can provide more profitable strategy for participating in open market. The MGCC buys power during low-price periods of the market and uses the capacity of the reformer to produce hydrogen for storage. This stored hydrogen can be used to produce electrical power and be sold to the market in high-price intervals. This strategy can make a good profit for the MG especially in reducing operational cost.

In order to verify impacts of the hydrogen management and thermal recovery on the efficiency of the FCPP Fig. 10 is given. To clarify the point two cases are defined. In the first case, neither hydrogen production management nor thermal energy recovery is considered while in the second one both of them are considered. As shown Fig. 10, hydrogen production management and thermal power recovery improve the overall efficiency of the FCPP greatly.

In order to make better sense of what is happening Table 4 is given. The detailed information and power balances of some hours are tabulated in this table. This information are regarding to best

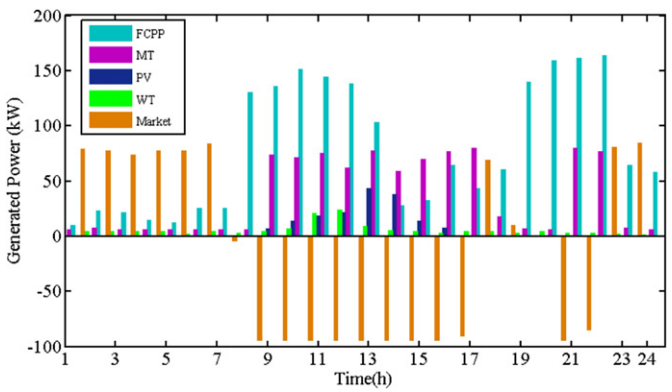

Fig. 8. Minimum cost – generated electrical power of different DER units.

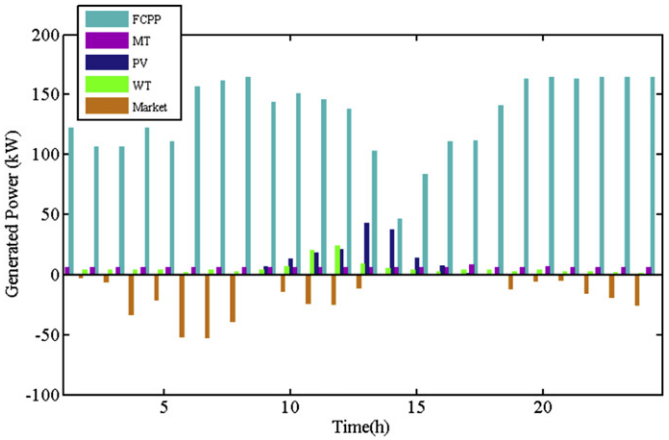

Fig. 9. Minimum emission – generated electrical power of different DER units.

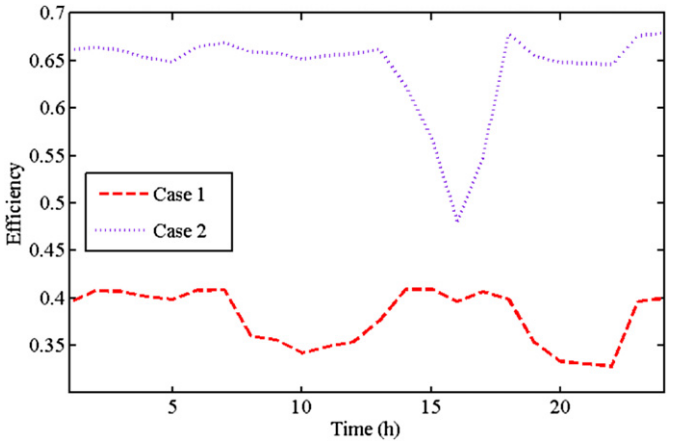

Fig. 10. FCPP efficiency plots.

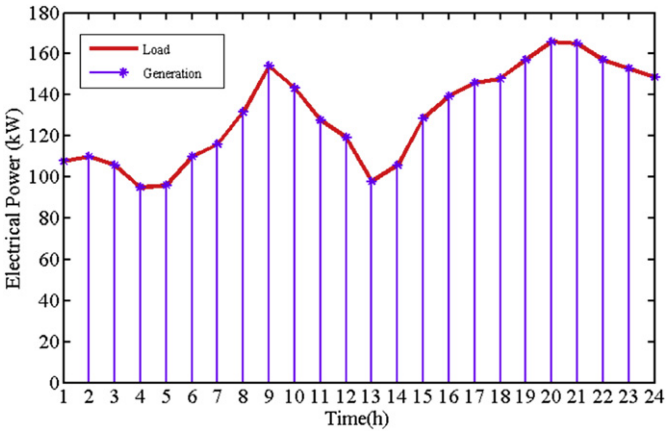

Fig. 11. Electrical load and generation for all simulations.

cost considering S_2. The design parameters of fuel cell are considered λ and i_{FC}. λ is an adjustable parameter which shows the membrane humidity. This parameter depends on the preparation procedure of the membrane and can be regulated by the relative humidity and Stoichiometry ratio of the anode feed gas. i_{FC} is cell operation current. Once λ and i_{FC} are explored based on the formulations given in Ref. [4], P_{cell} can be calculated. For the other DGs active power is considered as design variables. Analyzing this table shows how electrical and thermal load are fulfilled. Furthermore, Fig. 11 shows the electrical load and generation for all members of the POFs portrayed in Fig. 3. As shown this figure electrical load demands of all hours are fulfilled satisfactorily.

8.2. Probabilistic analysis

In the deterministic analysis, it is assumed that all IRVs values are equal to their forecasted values. However, as discussed in the pervious sections some required data for the EEM can't forecasted exactly. For example, wind and solar power have stochastic nature. Moreover, in the open access market, there are always errors in forecasted values for power market and fuel prices. Likewise, the load demands are more unpredictable than before. As a result, the solutions of the deterministic optimization algorithms discussed in the previous subsection are not reliable in the new circumstance.

In this section, the $2m + 1$ point estimate method is implemented along with the multi-objective MGSA to find the POF of the probabilistic EEM problem. The data considered as the uncertain inputs are as: electrical and thermal load demands, available output power of the PV and WT units, market prices in each interval, natural gas price for the FCPP, operation temperature of the FC, pressure of the reactant gases of FC, fuel price for the thermal loads of the MG which are not satisfied by the FCPP and hydrogen selling price. The normal distribution is assumed for all IRVs except output power of WT unit which is modeled by the Beta PDF [25,42].

Fig. 12 shows the POF of the probabilistic EEM problem found by the MGSA linked to the $2m + 1$ point estimate method. Referring to Fig. 12, the proposed approach successfully found uniformly POF. The DM based on his/her preference and priorities selects one of the members of the Pareto-optimal solutions. Figs. 13 and 14 portray the cumulative density functions (CDFs) of the cost and emission for three POF solutions (marked in Fig. 12). The Gram–Charlier is employed to find the accurate distribution for total operational cost and emission. Figs. 13 and 14 demonstrate that the proposed probabilistic approach could successfully describe the variations of the cost and emission which are the consequence of the variations of the IRVs. It also helps the system operators to know how likely uncertainties affect the system and how to handle the related issues.

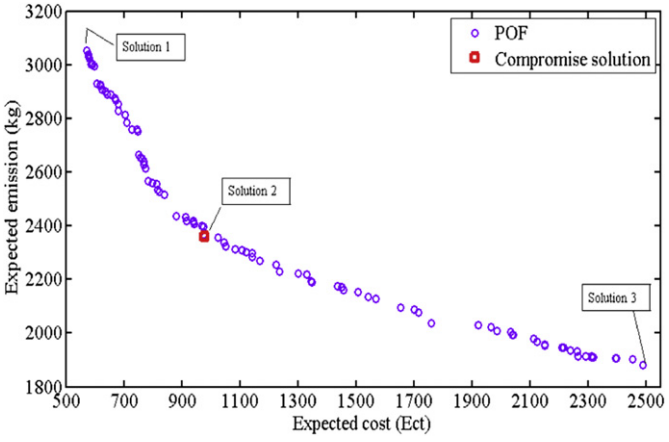

Fig. 12. POF of the probabilistic EEM problem.

Table 4
Detailed information for some hours regarding to best cost scenario 2.

	FCPP			MT	PV	WT	Market	Boiler	Recovered thermal energy	Thermal load	Electrical load
	i_{FC}	λ	P_{cell}								
1st hour	1.21	9.51	9.94	6.06	0	4.17	91.84	93.32	6.68	100	112
2nd hour	3.02	18.96	23.08	7.34	0	4.17	79.42	29.83	73.17	103	114
21st hour	27.78	10.17	161.69	79.88	0	3.03	−94.81	4.01	155.99	160	168
22nd hour	28.59	13.81	163.96	76.68	0	3.03	−85.77	10.53	159.47	170	160
23rd hour	9.34	9.74	64.31	7.60	0	2.14	80.56	129.53	46.47	176	155
24th hour	8.32	10.43	57.96	6.00	0	1.44	84.58	133.78	41.22	175	150

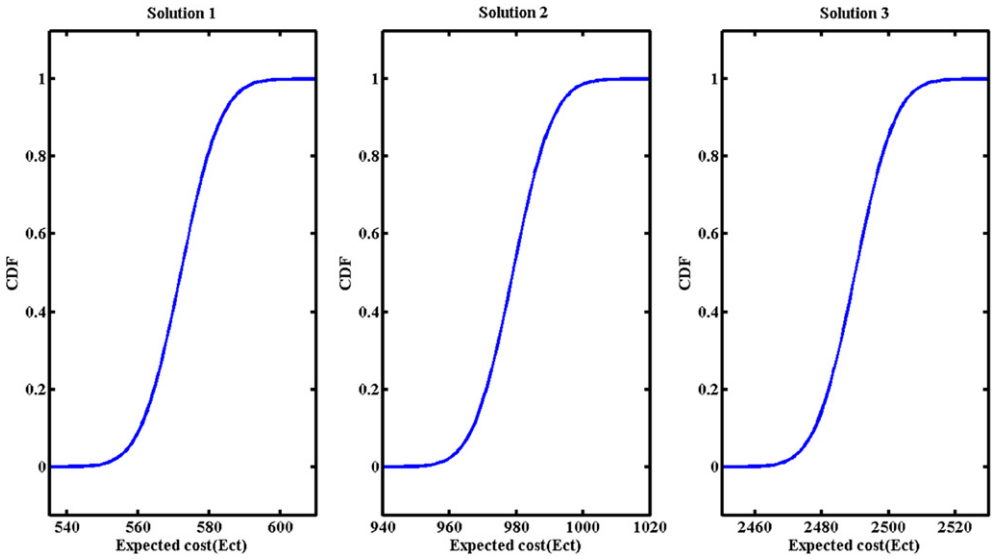

Fig. 13. CDF of the expected cost.

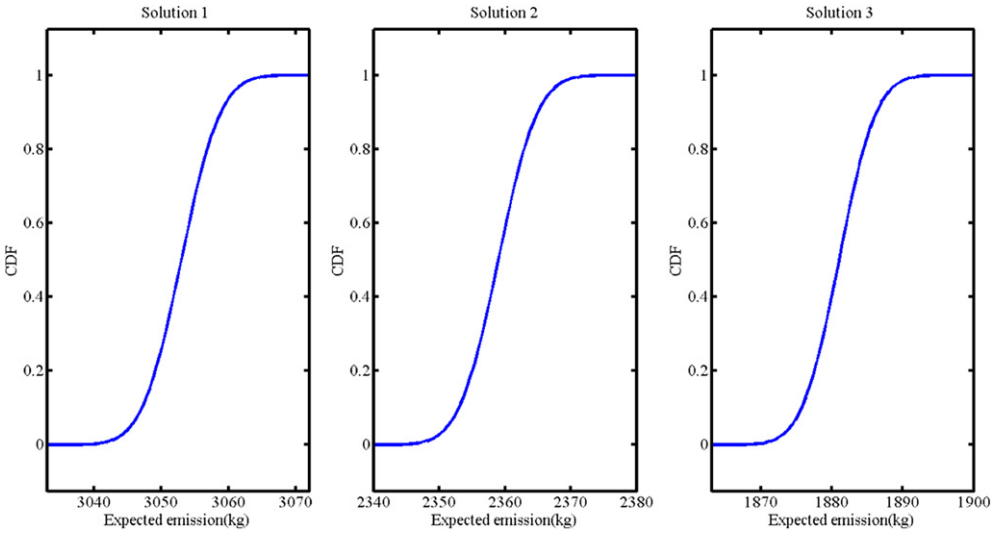

Fig. 14. CDF of the expected emission.

Finally, to verify the impact of the considering uncertainty in the decision making, the value of the stochastic solution (VSS) [43] is calculated. The VSS represents how much the MGCC would be willing to spend in order to know the future realization of the problem and cover the uncertainty in the stochastic processes under consideration. The VSS is calculated by subtracting the expected cost (output of the deterministic EEM problem) from the output of the stochastic model. The VSS is calculated 18 (€ct) in this test.

9. Conclusion

In this paper, a probabilistic approach for modeling and solving the EEM problem of renewable MGs under uncertain environment was proposed. In the proposed model, the hydrogen production and utilization management, the thermal energy recovery and trade with the upstream grid were employed along with different DERs to satisfy the thermal and the electrical load simultaneously. The thermal energy produced by the reformer was recovered while the thermal energy of the FC stack was neglected. This paper emphasized particularly the PEMFCs and organized the economic/emission model based on an electrochemical model of them. A multi-objective MGSA was proposed and linked to the $2m+1$ point estimate method to find uniformly POF of the EEM problem. In order to verify the impact of the hydrogen production on the EEM problem two scenarios were defined. One of them considered the hydrogen management while the other one neglected it. The simulation results showed the great improvement which the hydrogen production and utilization management could offer. The enhancements in both cost and emission minimization were discussed. In addition, the results showed that the hydrogen management and thermal recovery could provide 30–35% increase in the efficiency of the FCPP. Moreover, the simulation results demonstrated that the optimization algorithm force the MG to store some amount of produced hydrogen in high thermal load intervals and use it to generate electricity in low thermal load intervals. By this policy, less thermal power would be wasted, so more money and emission could be saved. Finally, to cover different

uncertainties in the EEM problem, the IRVs are modeled by the Beta and normal distributions and the probabilistic POF of the EEM problem was found. The CDF of three members of the probabilistic POF were portrayed. The figures showed that the proposed probabilistic approach could successfully describe the variations of the cost and emission which follow the variation of the IRVs. It also helps the system operators to know how likely uncertainties affect the system and how to handle the related issues.

References

[1] G. Venkataramanan, C. Marnay, IEEE Power Energy Mag. 6 (2008) 78–82.
[2] F. Katiraei, R. Iravani, N. Hatziargyriou, A. Dimeas, IEEE Power Energy Mag. 6 (2008) 54–65.
[3] C. Ziogou, D. Ipsakis, C. Elmasides, F. Stergiopoulos, S. Papadopoulou, P. Seferlis, S. Voutetakis, J. Power Sources 196 (2011) 9488–9499.
[4] J. Corrêa, F. Farret, L. Canha, M. Simões, IEEE Trans. Ind. Electr. 51 (2004) 1103–1112.
[5] G. Masters, Renewable and Efficient Electric Power Systems, third ed., John Wiley & Sons, Inc, 2004.
[6] J.C. Amphlett, R.F. Mann, B.A. Peppley, P.R. Roberge, A. Ro-drigues, J. Power Sources 61 (1996) 183–188.
[7] M.Y. El-Sharkh, A. Rahman, M.S. Alam, J. Power Sources 139 (2005) 165–169.
[8] N.V. Gnanapragasam, B.V. Reddy, M.A. Rosen, Int. J. Hydrogen Energy 35 (2010) 4788–4807.
[9] A. Ajanovic, Int. J. Hydrogen Energy 33 (2008) 4223–4234.
[10] A. Balabel, M.S. Zaky, Int. J. Hydrogen Energy 36 (2011) 4653–4663.
[11] R.A. Costa, J.R. Camacho, J. Power Sources 161 (2006) 1176–1182.
[12] C.-E. Hubert, P. Achard, R. Metkemeijer, J. Power Sources 156 (2006) 64–70.
[13] A.G. Tsikalakis, N.D. Hatziargyriou, IEEE Trans. Energy Convers. 23 (2008) 241–248.
[14] R. Chedid, S. Raiman, IEEE Trans. Energy Convers. 12 (1997) 79–85.
[15] M.Y. El-Sharkh, M. Tanrioven, A. Rahman, M.S. Alam, Int. J. Hydrogen Energy 35 (2010) 8804–8814.
[16] B. Shabani, J. Andrews, Int. J. Hydrogen Energy 36 (2011) 5442–5452.
[17] H. Ren, W. Gao, Energy Buildings 42 (2010) 853–861.
[18] A.D. Hawkes, D.J.L. Brett, N.P. Brandon, Int. J. Hydrogen Energy 34 (2009) 9545–9557.
[19] A.D. Hawkes, D.J.L. Brett, N.P. Brandon, Int. J. Hydrogen Energy 34 (2009) 9558–9569.
[20] A.D. Hawkes, M.A. Leach, Energy 32 (2007) 711–723.
[21] A. Soroudi, M. Ehsan, R. Caire, N. Hadjsaid, Trans. Power Syst. 4 (2011) 2293–2301.
[22] A. Soroudi, M. Aien, M. Ehsan, IEEE Syst. J. 99 (2011) 1–10.
[23] J. Hethey, S. Leweson, Master thesis, Technical University of Denmark, 2008.
[24] G.J. Anders, Wiley, New York, 1990.
[25] J.M. Morales, J. Perez-Ruiz, IEEE Trans. Power Syst. 22 (2007) 1594–1601.
[26] R.Y. Rubinstein, Wiley, New York, 1981.
[27] C.-L. Su, IEEE Trans. Power Syst. 20 (2005) 1843–1851.
[28] A.R. Malekpour, T. Niknam, Energy 36 (2011) 3477–3488.
[29] E. Rashedi, H. Nezamabadi-pour, S. Saryazdi, Inf. Sci. 179 (2009) 2232–2248.
[30] A. Moghaddam, A. Seifi, T. Niknam, M.R. Pahlavani, Energy 36 (2011) 6490–6507.
[31] P. Mago, A. Hueffed, Energy Buildings 42 (2010) 1628–1636.
[32] S. Campanari, E. Macchi, G. Manzolini, Asia-Pacific J. Chem. Eng. 4 (2009) 301–310.
[33] L. Wang, A. Husar, T. Zhou, H. Liu, Int. J. Hydrogen Energy 28 (2003) 1263–1272.
[34] E. Rosenblueth, Proc. Natl. Acad. Sci. U.S.A. 72 (1975) 3812–3814.
[35] E. Harr, Appl. Math. Model. 13 (1989) 313–318.
[36] H.P. Hong, Reliab. Eng. Syst. Saf. 59 (1998) 261–267.
[37] P. Zhang, S.T. Lee, IEEE Trans. Power Syst. 19 (2004) 676–682.
[38] D. Holliday, R. Resnick, J. Walker, John Wiley and Sons, 1993.
[39] M.A. Abido, Electr. Power Energy Syst. 25 (2003) 97–105.
[40] A. Anvari Moghaddam, A.R. Seifi, IET Renew. Power Gen. 5 (2011) 470–480.
[41] T. Niknam, E. Azad-Farsani, M. Nayeripour, B. Firouzi, Euro. Trans. Electr. Power 21 (2011) 201–209.
[42] A. Fabbri, T. Román, J. Abbad, V. Quezada, IEEE Trans. Power Syst. 20 (2005) 1440–1446.
[43] J.M. Morales, Ph.D. dissertation, Dept. Electr. Eng., Univ. Castilla-La Mancha, Ciudad Real, Spain, 2010.